Hydrophobic Collapse of Foldamer Capsules Drives Picomolar-Level Chloride Binding in Aqueous Acetonitrile Solutions

Yuran Hua, Yun Liu, Chun-Hsing Chen, and Amar H. Flood*

Department of Chemistry, Indiana University, 800 East Kirkwood Avenue, Bloomington, Indiana 47405, United States

Ⓢ Supporting Information

ABSTRACT: Aqueous media are competitive environments in which to perform host−guest chemistry, particularly when the guest is highly charged. While hydrophobic binding is a recognized approach to this challenge in which apolar pockets can be designed to recognize apolar guests in water, complementary strategies are required for hydrophilic anions like chloride. Here, we present evidence of such an alternative mechanism, used everyday by proteins yet rare for artificial receptors, wherein hydrophobic interactions are shown to be responsible for organizing and stabilizing an aryl-triazole foldamer to help extract hydrophilic chloride ions from increasingly aqueous solutions. Therein, a double-helical complex gains stability upon burial of ~80% of the π surfaces that simultaneously creates a potent, solvent-excluding microenvironment for hydrogen bonding. The chloride's overall affinity to the duplex is substantial in 25% water v/v in acetonitrile (log β_2 = 12.6), and it remains strong (log β_2 = 13.0) as the water content is increased to 50%. With the rise in predictable designs of abiological foldamers, this water-assisted strategy can, in principle, be utilized for binding other hydrophilic guests.
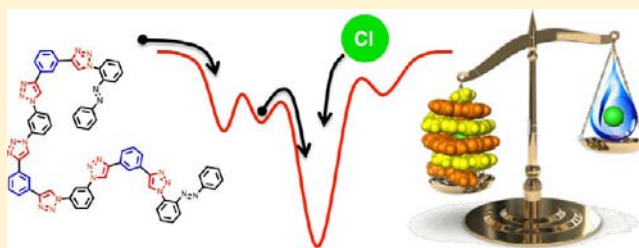
INTRODUCTION

Chemists have made significant advances toward the recognition of various molecules across a range of environments ever since Pedersen,[1] Lehn,[2] and Cram[3] demonstrated that synthetic receptors could bind ions and molecules at the levels of affinity achieved by proteins.[4] Of continued interest is the binding of guests in aqueous media,[5−10] particularly for applications that may be of importance to human biology.[11] Hydrophobic interactions[12] provide a powerful driving force to aid in this goal. For instance, Diederich defined apolar cavities within water-soluble cyclophanes for complexing benzene-based guests.[13] However, when the guest is not hydrophobic, such as the highly hydrated and biorelevant[14] Cl− anion, strategies differing from like-dissolves-like are called for. In a recent review[15] examining the extraction of anions from mixed organic−aqueous solutions into synthetic receptors, positive charges[16−18] in rigidly organized hosts were considered a safe combination. Neutral hydrogen-bond donors in more flexible structures would therefore appear to be a riskier prospect, yet not without precedent. Groundbreaking studies by Kubik using cyclopeptides[19] and Jeong with indolo foldamers[20] gave Cl− affinities up to 10³ M−¹ (millimolar binding) and implicated hydrophobic driving forces[21] in helping to organize the complexes. Such behavior finds common currency with hydrophobic collapse in proteins.[22] If such an approach were general, it could be far-reaching. For instance, by using hydrophobic collapse, chemists can create a microenvironment of low dielectric constant, ε,[23−25] that would strengthen any hydrogen bonds[26] set into the receptor's core. Inspired by these former examples and motivated by protein folding, we designed

aryl-triazole foldamers (Figure 1) for binding Cl− in a solvent-excluding pocket. We were surprised to discover the formation of a 2:1 duplex displaying an unprecedented Cl−-bound stability of $\beta_2 > 10^{12}$ M−² (picomolar concentrations) in 50% v/v water/ acetonitrile (MeCN), and we show conclusively that hydrophobic collapse offsets the penalty of dehydrating Cl−.

Toward the binding of Cl− in pure water or in mixed aqueous solutions, the receptor needs to incorporate features to overcome the large penalty associated with dehydrating the anion, $\Delta G_{hyd}(Cl^-) = 340$ kJ mol−¹.[27] Another way to gauge this penalty is to consider the free energy of transferring Cl− from water to an aprotic solvent like acetonitrile, $\Delta G_{water \rightarrow MeCN}(Cl^-)$ = +42 kJ mol−¹.[27] This cost indicates that an affinity of ~10⁷ M−¹ in MeCN would be reduced to zero in water when all other factors are equal, but, as elaborated in this paper, this is not always the case. In contrast to Cl−, charge-diffuse anions like I− and ClO₄− do not face similar dehydration penalties,[28] and they can be extracted into apolar cavities with increasing affinity following the Hofmeister bias.[29−31] Charge-dense Cl− ions remain a challenge. Yet, Nature readily and routinely extracts them and others[32] from their hydration shells, if only temporarily, into neutral binding environments as they pass through transmembrane channels. Chloride regulation across lipid membranes facilitates a range of processes[33] from muscle excitation to organelle acidification and is implicated in diseases like cystic fibrosis.[14] Crystal structures of ClC chloride channels[34] show the bound Cl− ion inside a binding pocket
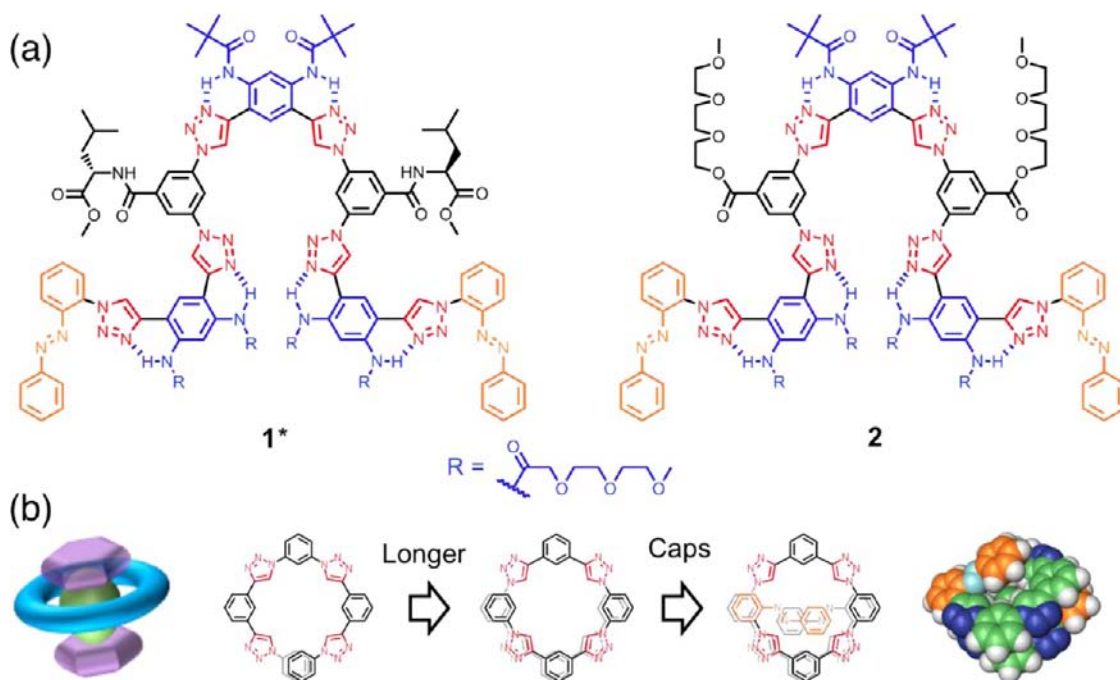
Figure 1. (a) Chemical structures of aryl-triazole foldamers bearing side chains for optical activity (1*) and broader solubility (2). Color coding: CH hydrogen-bonding triazoles, red; preorganizing *exo*-amides, blue; chiral or solubilizing groups, black; and azobenzene caps, orange. (b) General design pathway to create a capped receptor (left) using a foldamer platform; (right) molecular model of the expected compact structure.

that is separated from a water-accessible region by ∼5 Å, which helps create a favorable microenvironment. The Cl⁻ is stabilized by the electropositive ends of three α-helix macrodipoles and held in place by multiple hydrogen bonds: two short OH···Cl⁻ contacts, $d_{\text{O···Cl}}$ = 3.1 and 3.2 Å, two short NH···Cl⁻ contacts, $d_{\text{N···Cl}}$ = 3.4 and 3.5 Å, plus longer CH-based contacts, $d_{\text{C···Cl}}$ = 3.7 and 3.8 Å.

Hydrophobic collapse is implicit to the structure and function of proteins. Transferring this concept to the organization of receptors for guest binding could be straightforward when applied using abiological foldamers;[35] they have predictable and solvent-programmable[36] conformations and have already been used extensively as a platform for molecular recognition.[37,38] While the possibility of hydrophobic organization has been appreciated for some time,[36] it has only been exploited recently for binding polar guests in aqueous solutions, like D-fructose.[39] Returning to anion recognition,[38,40,41] Jeong's water-soluble indolocarbazole foldamer[20] comprised large aromatic surfaces, allowing hydrophobic and π-stacking interactions to stabilize the helix in water. With six NH donors pointing into the cavity, Cl⁻ ions were found to be extracted from deuterated water with an association constant of 65 M⁻¹. While hydrophobic forces are implicit to the folded structure, an explicit signature verifying the role of hydrophobic interactions in the actual foldamer−guest binding process was not determined.

With these precedents in mind, we envisioned (Figure 1b) a capsule-like aryl-triazole foldamer for creating a solvent-excluding binding pocket. The overall capsule morphology takes its inspiration from Huc's molecular apple peels.[42] Beyond ongoing work with aryl-triazole receptors[43−45] and with foldamers,[46−50] we were also motivated by qualitative reports by Hecht[51] and Jiang[52] showing that similar, albeit solvent-exposed, foldamers could interact with Cl⁻ in aqueous solutions. In the first case,[51] addition of Cl⁻ induced helical

inversion, while in the second case,[52] Cl⁻ ions helped break up aggregates in aqueous solutions. In neither case were the association constants characterized. Here, we characterize affinities as a function of water content from pure MeCN to 25% and 50% water, the limit of the compounds' solubility. From a crystal structure, we see Cl⁻ binding in the center of the capsular foldamer as a single helix with 1:1 stoichiometry. We observe Cl⁻ binding by the 1:1 helix drop as hydration increases, an outcome typical of hydrophilic anions, for example, as seen with Kubik's cyclopeptides binding to sulfate.[21c] However, we discovered that this penalty could be offset during formation of a putative duplex with 2:1 stoichiometry, which showed enhanced stability with increased water content akin to the unambiguous signature of hydrophobic interactions observed by Kubik[21c] and Diederich.[53] As a consequence, two features emerge that are unprecedented in anion recognition.[15,54] First, the overall stability remains relatively unperturbed in increasingly aqueous media, and second, the Cl⁻ affinity (>10¹² M⁻²) is the strongest on record for a neutral system. These results deepen our understanding of this biomimetic strategy[55] and demonstrate its use in the design of functional abiological folded molecules in aqueous media.

■ RESULTS AND DISCUSSION

Molecular Design. Two aryl-triazole foldamers (1* and 2, Figure 1) based on a single backbone were designed to form chloride-binding pockets. Six triazoles (red) provide activated CH hydrogen-bond donors,[56] and the five phenylenes contribute supporting hydrogen bonds.[57] After folding, five π−π contacts between overlapping ends of the oligomer were incorporated to give a foundation for hydrophobic organization. Intramolecular hydrogen bonds from *exo*-amide groups (blue) were introduced to help lock[43k] 6 of the 12 rotatable aryl-triazole C−C bonds into conformations conducive for folding. Azobenzene-derived caps (orange) were selected to act as

Scheme 1. Synthesis of Azobenzene End-Cap 12[a]
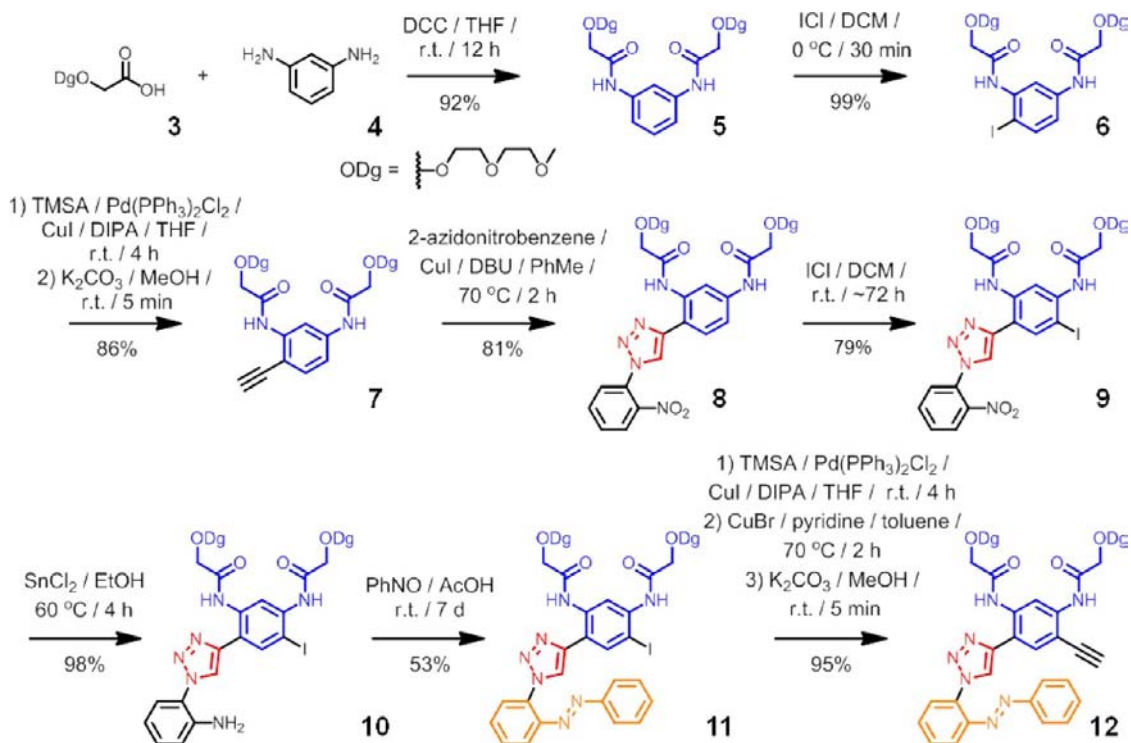
[a]Abbreviations: DCC, *N,N'*-dicyclohexylcarbodiimide; TMSA, trimethylsilylacetylene; DIPA, diisopropylamine; DBU, 1,8-diazabicycloundec-7-ene.

Scheme 2. Syntheses of Foldamers 1* and 2
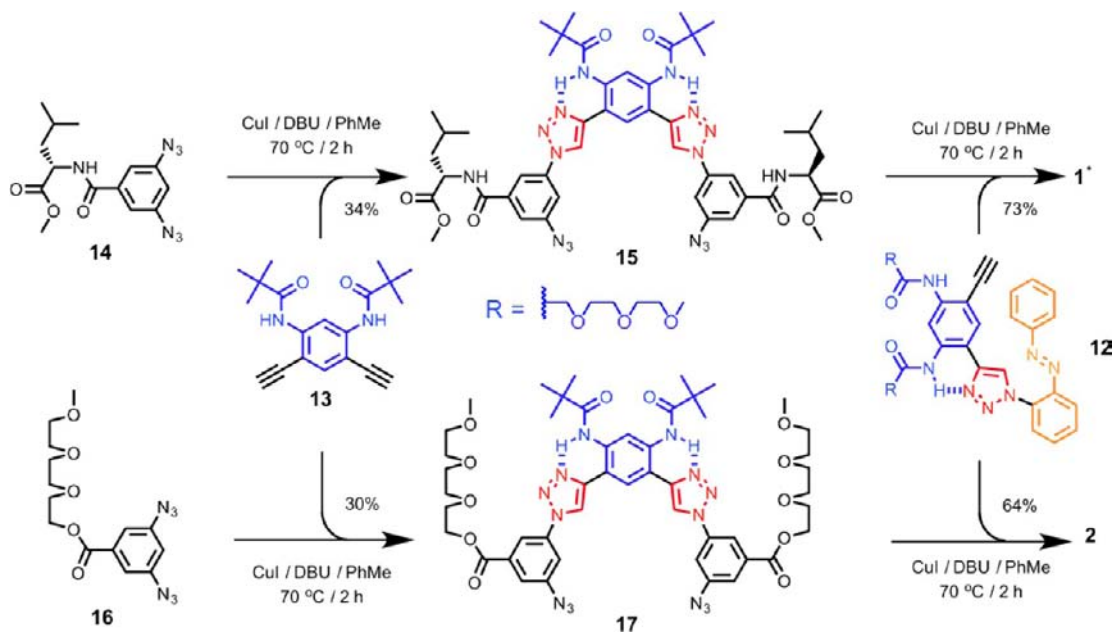
photoisomerizable gates that cover the solvent-exposed area of the foldamer, thus excluding solvent from the binding site. An *ortho*-linked azobenzene was used to direct the terminal benzene rings over the top and bottom of the binding pocket, in contrast to the *meta* linkages utilized previously in foldamers,[58,59] and for photodriven binding and release of chloride[43g,m] in solvent-exposed systems. Foldamer 1* bears chiral L-leucine-derived side chains to facilitate analysis of helically folded states[60] by using circular dichroism (CD) spectroscopy. Foldamer 2 bears ethylene glycol side chains for

greater solubility in more aqueous solutions, up to 50% v/v water in MeCN.

Foldamers 1* and 2 were synthesized in a convergent manner from the azobenzene-derived caps, 12 (Scheme 1), and the appropriate diazido-substituted pentads, 15 and 17, respectively (Scheme 2). Surprisingly, the ^{1}H NMR spectra of both foldamers recorded in CD$_2$Cl$_2$ after chromatographic purification (SiO$_2$ and Al$_2$O$_3$) displayed sharp resonances (1*, Figure S11a, and 2, Figure 2) rather than the broad features typically seen for empty aryl-triazole foldamers.[43b,g,51,52] This
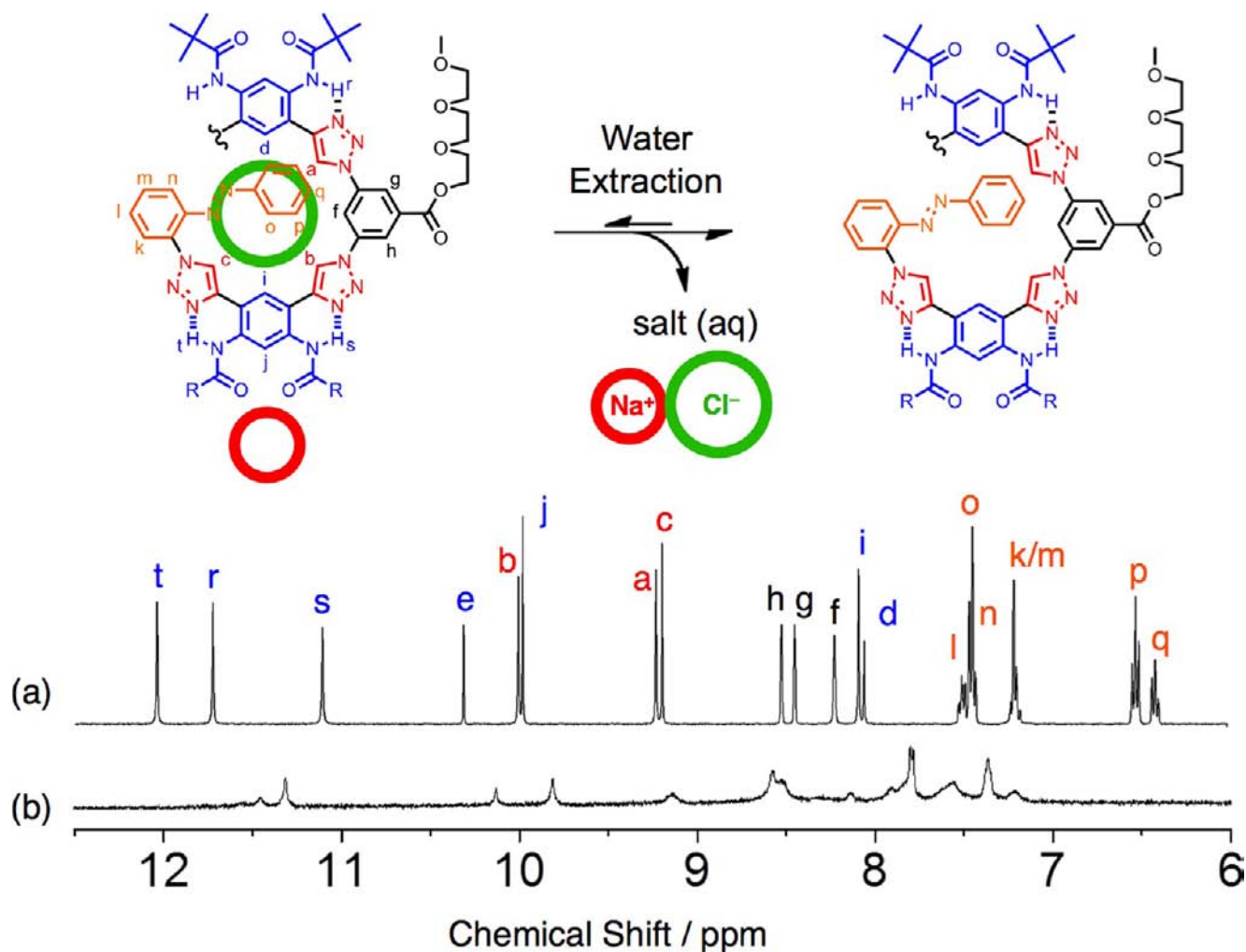
Figure 2. (a) ^{1}H NMR spectrum and peak assignments of the aromatic protons of foldamer $2 \cdot Cl^- \cdot Na^+$ (CD$_2$Cl$_2$, 500 MHz, 298 K). (b) Spectrum recorded after salt extraction from a CD$_2$Cl$_2$ solution using D$_2$O with sonication.

result suggests that the purified compounds emerged as chloride complexes. Based on titrations with various Cl$^-$ salts (*vide infra*), the complex appears to be saturated with 1 equiv or more of chloride. No salts were added to the elution solvents (CH$_2$Cl$_2$:MeOH = 100:6) nor the reaction solutions, and the CuI used in the reaction is present in too low amounts to effect saturation. Consequently, we believe the salt was extracted from the column support material during the chromatography. Consistently, extraction of the salt using water generated broad NMR spectra (**2**, Figure 2b). To the best of our knowledge, no other aryl-triazole receptors have extracted a salt from silica support material, providing an early indication of the foldamer's chelating strength.

Structures of 1:1 Foldamer Complexes in the Solid State and Solution. Recrystallization of **1*** from MeCN resulted in single crystals suitable for X-ray diffraction analysis. The solid-state structure of $1^* \cdot Cl^- \cdot Na^+$ (Figure 3) confirms the composition of the complex, the identity of the salt, and the presence of the design elements inscribed into the foldamer's structure. The foldamer adopts an *M*-helical conformation, which is amplified into a 1D helix by a 4_3 screw axis in the solid state that is assisted by hydrogen bonds between L-leucine fragments of neighboring foldamers (see Supporting Information). The chloride ion is sitting inside the binding pocket with azobenzene caps defining a capsule. The sodium ion is located

within the two acyclic polyethers that come together from two slip-stacked phenylenes, whose presence is reminiscent of crowns[1] interacting with alkali cations. The chloride ion is stabilized by 11 CH···Cl$^-$ hydrogen bonds (Figure 3c). Six short contacts involve four of the triazoles with two at a distance of $d_{C\cdots Cl} = 3.4$ Å and two at 3.5 Å, which match the NH···Cl$^-$ hydrogen bonds seen in the ClC protein,[34] plus two phenylene ones at 3.7 Å. In addition, there are five longer contacts coming from two triazoles at 3.9 Å and three phenylenes at 4.0 Å. The four shortest hydrogen bonds, $d_{H\cdots Cl} = 2.52, 2.53, 2.55,$ and 2.56 Å are all far beneath the sum of the van der Waals contacts (2.95 Å). They match well with the triazole-based CH···Cl$^-$ hydrogen-bond length of 2.6 Å seen in the crystal structure of a pentad structure[61] and the 2.4 Å seen in a gas-phase calculation, B3LYP/6-31+G(d,p), on a pentad.[43k]

The well-resolved ^{1}H NMR spectrum (Figure 2) of $2 \cdot Cl^- \cdot Na^+$ allows the solution-phase structure to be evaluated. Resonances in the aromatic region were assigned (see Supporting Information) on the basis of their peak integrations, cross-peaks identified in the 2D NOESY (Figure 4), and chemical environment. Verifying formation of CH···Cl$^-$ hydrogen bonds,[43] the three triazole CH resonances (a, b, c) all appeared above 9 ppm. While the three phenylene CH hydrogen-bond donors are not shifted downfield as much as
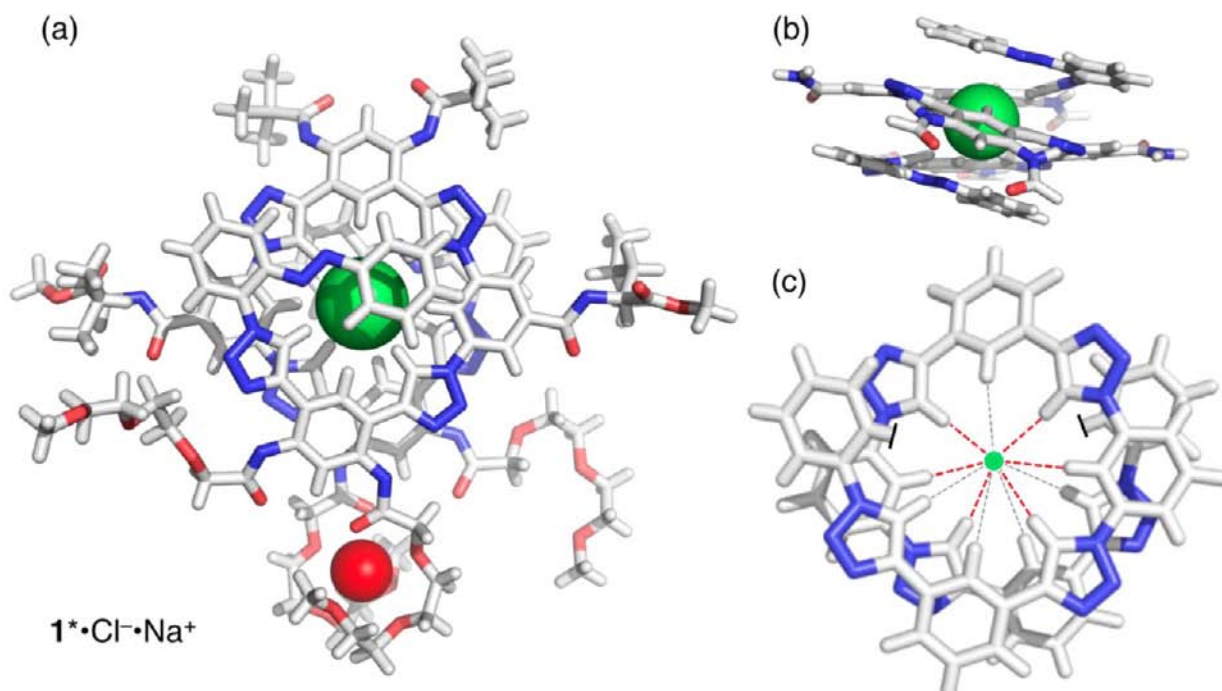
Figure 3. (a) Crystal structure of $1^*\cdot Cl^-\cdot Na^+$ emphasizes azobenzene caps and the ion-pair complexation of Cl^- (green ball) and Na^+ (red ball), with (b) the side view highlights the *M* helix (side chains removed for clarity). (c) View of the chloride-binding pocket with the side chains and azobenzene caps removed to visualize the 11 $CH\cdots Cl^-$ hydrogen-bonding contacts. Thick red lines are short contacts (triazoles 2.52−2.56 Å, phenylenes 2.79 and 2.85 Å), and thin gray lines are longer contacts (2.93−3.21 Å).

the triazoles, the shortest of their $CH\cdots Cl^-$ contacts in the solid state involves a hydrogen (f) that is more deshielded than the other two (d, i). Diagnostic cross-peaks (see magenta boxes and inset to Figure 4) between the azobenzene proton (o) and the intracavity protons (b, c, i) indicate that the salt-bound foldamer $2\cdot Cl^-\cdot Na^+$ likely adopts a conformation in solution similar to that of the chiral foldamer $1^*\cdot Cl^-\cdot Na^+$ in the solid state.

Preorganization of the Empty Foldamers. CD spectroscopy of the empty oligomer 1^* in MeCN was characterized in order to shed some light on the level of preorganization of the binding pocket. Prominent features in the 250−400 nm region (Figure 5, black line) indicate the foldamer has some degree of chiral induction from the L-leucine substituents. The negative peak centered at 275 nm has been observed in the CD spectra of a related foldamer;[43g] consequently, it is attributed to the aryl-triazole backbone. The features at 325 and 350 nm may also arise from the backbone instead of the azobenzene moieties. This assignment is strengthened by the fact that they barely change upon isomerization of the azobenzenes with UV light (see Supporting Information) to a photostationary state with a modest ~35:65 *cis*-to-*trans* ratio (see Supporting Information). In 50:50 MeCN:H$_2$O, corresponding CD features of 1^* increased at the beginning until 0.5 equiv of Cl^- was added (Figure 5b), at which point most CD signals began to decrease in a similar fashion as those in pure MeCN (Figure 5a). No evidence was found for self-association of foldamer **2** in 50:50 MeCN:H$_2$O using a variable concentration UV−vis study from 0.8 to 58 μM (see Figure S30), indicating that even in a poor solvent, intermolecular aggregation does not play a role in the CD response at 5 μM. In the variable-concentration CD measurement, isosbestic points disappeared beyond 25 μM in CH$_3$CN (see Figure S31), indicating that any self-aggregation may only happen at higher concentrations.

Consistently, ^{1}H NMR spectra of 1^* and **2** (Figures S6 and S8, *vide infra*) recorded in CD$_3$CN at 1 mM show broadened resonances. All together, these data suggest that the binding pocket inside the empty foldamer is at least partially preorganized in a helical conformation at room temperature in MeCN. This situation contrasts with Jeong's indolocarbazole foldamers[20] in deuterated water, which appeared to be completely prefolded prior to addition of anions.

Solution-Phase Binding Behavior in Mixed Aqueous Solutions. The impact of water on the equilibria involving chloride binding was characterized in solutions containing 0%, 25%, and 50% v/v water in MeCN. Compared to pure MeCN, the additional penalties for desolvating chloride from the two aqueous solutions are 10.5 and 21 kJ mol^{-1}, respectively, as estimated from the free energy of transferring Cl^- ions between the two pure solvents.[27] The principal hypothesis under investigation is whether the design of this foldamer can offset this penalty.

Complexation was monitored using multiple techniques to first establish the dominant equilibria and associated species present in solution. The $1^*\cdot Cl^-\cdot Na^+$ and $2\cdot Cl^-\cdot Na^+$ salts were examined in addition to the complexes that are formed during addition of tetrabutylammonium chloride (TBACl) and tetraethylammonium chloride (TEACl). In addition to the 1:1 complex seen in the crystal structure and electrospray ionization mass spectra (ESI-MS) of $1^*\cdot Cl^-$ (2420.0422 m/z) and $2\cdot Cl^-$ (2460.0198 m/z), another complex with 2:1 foldamer:Cl^- stoichiometry was evident. For instance, a peak observed in the ESI-MS at ~4886 m/z is assigned to $2_2\cdot Cl^-$, and titrations show this species emerges when 0.5 equiv of Cl^- is added into solution. These observations suggested a model of key equilibria (Figure 6) to consider.

NMR spectra recorded during chloride titrations with the salt-free foldamers 1^* and **2** in various solvents suggest that
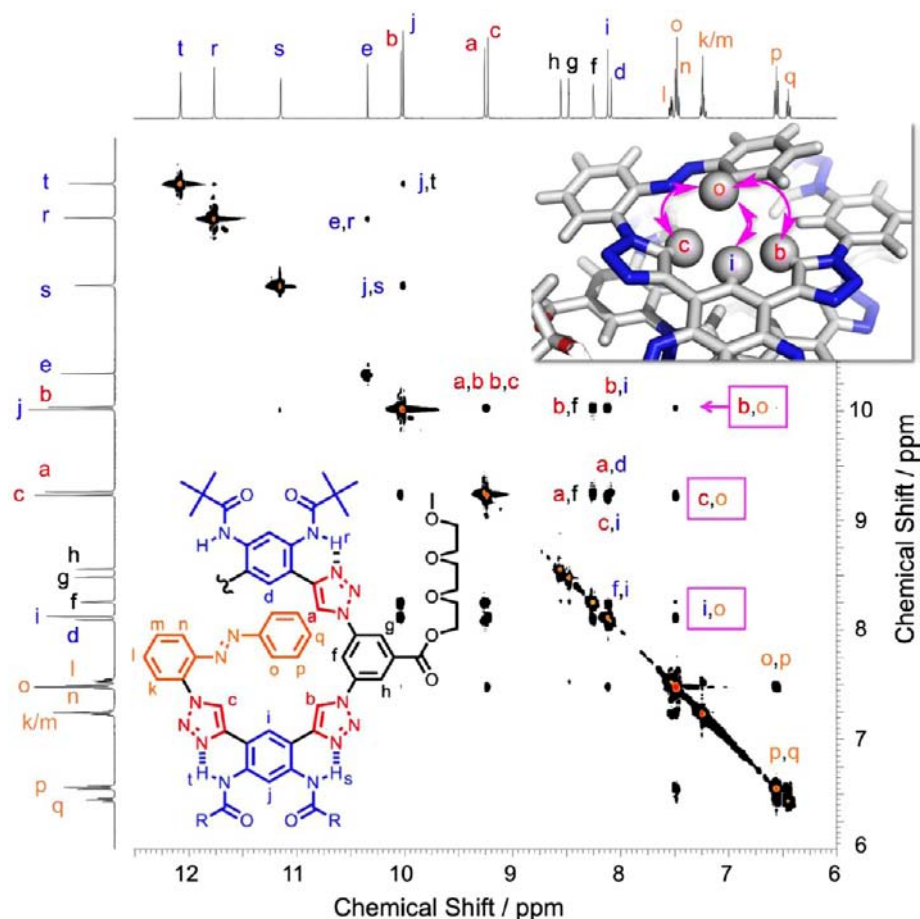
Figure 4. 2D NOESY spectrum of **2**·Cl⁻·Na⁺ (CD₂Cl₂, 500 MHz, 298 K) with key intramolecular cross-peaks marked (magenta) in relation to the crystal structure of **1***·Cl⁻·Na⁺ (inset).
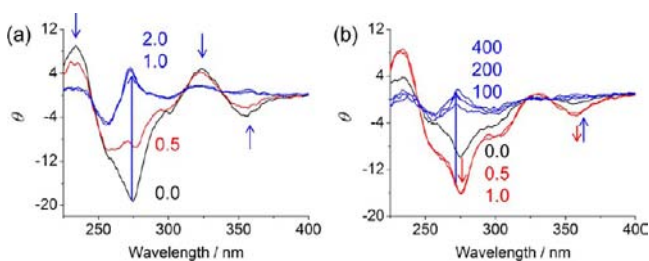
Figure 5. CD titrations of foldamer **1*** (5 μM) with TBACl in (a) MeCN (0−2 equiv) and (b) 50% MeCN:H₂O (0−400 equiv).

both foldamers behave similarly. Saturation of the receptors was achieved with the addition of less than 2 equiv of either TEACl or TBACl in CD₂Cl₂ to **1*** (Figure 7) and **2** (Figure S7). An intermediate species assigned to the duplex, **1***₂·Cl⁻, is observed in several resonances, marked by magenta boxes at ∼10.6, 9.6, 9.0, and 6.8 ppm, reaching their maximum intensities with 0.4−0.6 equiv of chloride (Figure 7). In addition, these resonances all appear at downfield positions when compared to corresponding resonances in the single helix, indicating a stronger shielding attributed to more significant π−π contacts in the duplex. Two sets of resonances is characteristic[62] of a 2:1 binding equilibrium in slow exchange with the single helix. Further support for the double−single helix assignments comes from diffusion NMR experiments (Figure S13). Therein, two solutions were analyzed with 0.5 and 2.0 equiv of TEACl present in order to access the turning

and end points, respectively, with reasonably sharp peaks to facilitate the experiment. Diffusion coefficients of $(3.8 \pm 0.2) \times 10^{-10}$ and $(5.2 \pm 0.1) \times 10^{-10}$ m² s⁻¹ correlated with a ratio between the volumes of the two species of 2.6 ± 0.5, based on the Stokes−Einstein equation and assuming they are spherical in shape. The ratio matches with single- and double-helical formations.

The peaks for the duplex were observed in the ¹H NMR spectrum following dissolution of **1***·Cl⁻·Na⁺ crystal in CD₂Cl₂ (Figure 7). These peaks can be distinguished from the single helix by comparison to the TEACl-saturated species. Thus, the CD₂Cl₂ solution of **1*** with 1 equiv of NaCl is also equilibrating slowly between the 1:1 and 2:1 complexes present at a 4:7 molar ratio. By contrast, adding 1 equiv of TEACl to the free foldamer **1*** shows a >95:5 molar ratio in favor of the single helix. This observation suggests that the Na⁺ countercation participates cooperatively in the stabilization of the putative 2:1 duplex. Presumably, the Na⁺ ion coordinates to the glycol side chains of the chloride complexes of **1*** in CD₂Cl₂, forming an ion-pair complex[63] in a manner that may resemble the solid-state structure.

The NMR resonances arising from both complexes in the region above 8.5 ppm were categorized (Figure 7) into three groups, facilitating an analysis of the average symmetry: amide protons Hʳ, Hˢ, and Hᵗ (12.2−10.5 ppm); *exo*-phenylene proton Hᵉ (∼10.3 ppm); and triazole protons Hᵃ, Hᵇ, Hᶜ in the same region as *exo*-phenylene proton Hʲ (10.2−8.9 ppm). All chemically equivalent protons for both complexes showed just

14406

dx.doi.org/10.1021/ja4074744 | *J. Am. Chem. Soc.* 2013, 135, 14401−14412
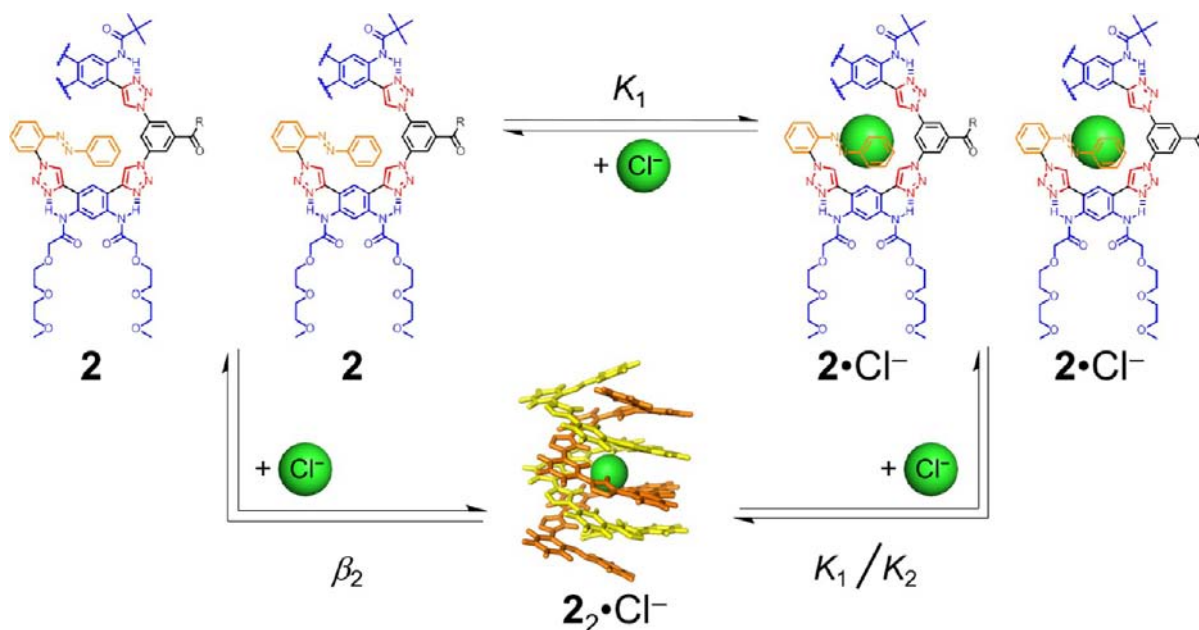
Figure 6. Key binding equilibria showing how the double helix can be accessed prior to the single helix during the titration with chloride into solutions. A molecular model of the double helix is presented with the side chains removed.
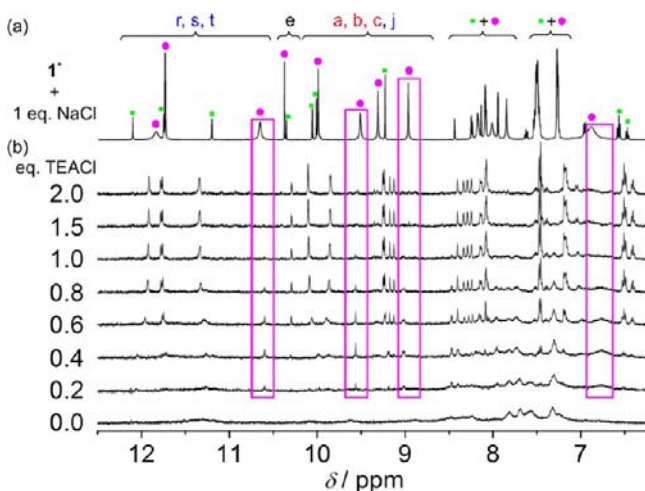
Figure 7. (a) ^{1}H NMR spectrum of $\mathbf{1}^*\cdot Cl^-\cdot Na^+$ crystals dissolved into CD_2Cl_2, with peak assignments for the 1:1 helical complex (small green squares) and the 2:1 duplex (large magenta circles). (b) Titration data recorded upon addition of TEACl to $\mathbf{1}^*$ in CD_2Cl_2 (2 mM, 500 MHz, 298 K), with resonances assigned to the duplex (0.2–0.8 equiv) marked using magenta boxes.

from different titrations showed similar patterns in the aromatic region (cf. Figures 2, S6, 7, and 8).
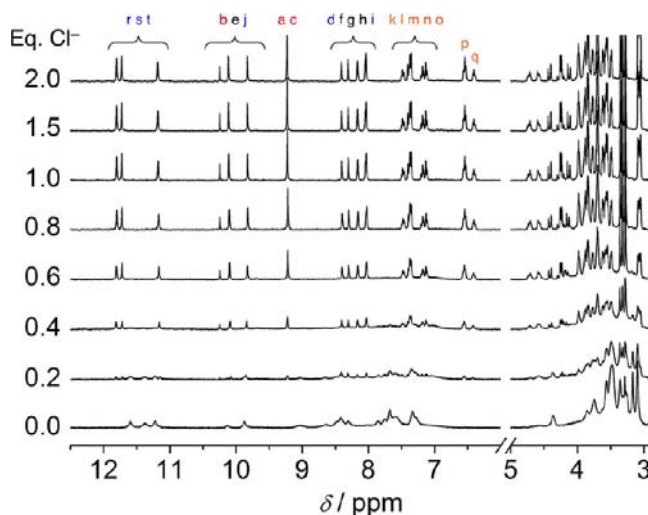
Figure 8. ^{1}H NMR titration of foldamer $\mathbf{2}$ (1 mM) in CD_3CN with TBACl (500 MHz, 298 K).

one set of resonances, e.g., three sets of singlets for three types of phenylene-based amide NH protons. This observation provides evidence that the time-averaged structure of the duplex $\mathbf{1}^*_2\cdot Cl^-$ in solution has the D_2 symmetry of an intertwined double helix. The broadened proton peaks suggest a dynamic behavior involving the interchange between two dissymmetrical conformers[48] with C_2 symmetry via a relative screw motion occurs at rates close to the NMR time scale.

Similar titration behaviors are seen across various conditions for $\mathbf{1}^*$ and $\mathbf{2}$. The foldamer's solubilizing group (chiral or glycol), the solvent used (CD_2Cl_2 or CD_3CN), and the countercation present (Na^+, TEA^+, or TBA^+) do not appear to affect the geometry of the chloride-binding sphere in the 1:1 complex on account of the fact that the final spectra obtained

The NMR titration of foldamer $\mathbf{2}$ with TEACl in aqueous solution (50:50 D_2O:CD_3CN, Figure S9) generated features for the 1:1 complex similar to those seen in the other solvents, with the exception that H/D exchange led to loss of the amide signals. Addition of 0.5 equiv of TEACl generated three new and poorly resolved aromatic peaks at 8.4, 7.1, and 6.6 ppm that remained largely unchanged until larger quantities of chloride (≥ 5 equiv) were introduced. From 10 to 400 equiv, resonances matching those seen for the other 1:1 complexes sharpened up and showed continued migrations.

The CD titration recorded at 5 μM (Figure 5) indicates that in aqueous solutions the system evolves from the empty foldamer, through a 2:1 duplex and out to the 1:1 complex, while in MeCN the 2:1 duplex is diluted away so that the
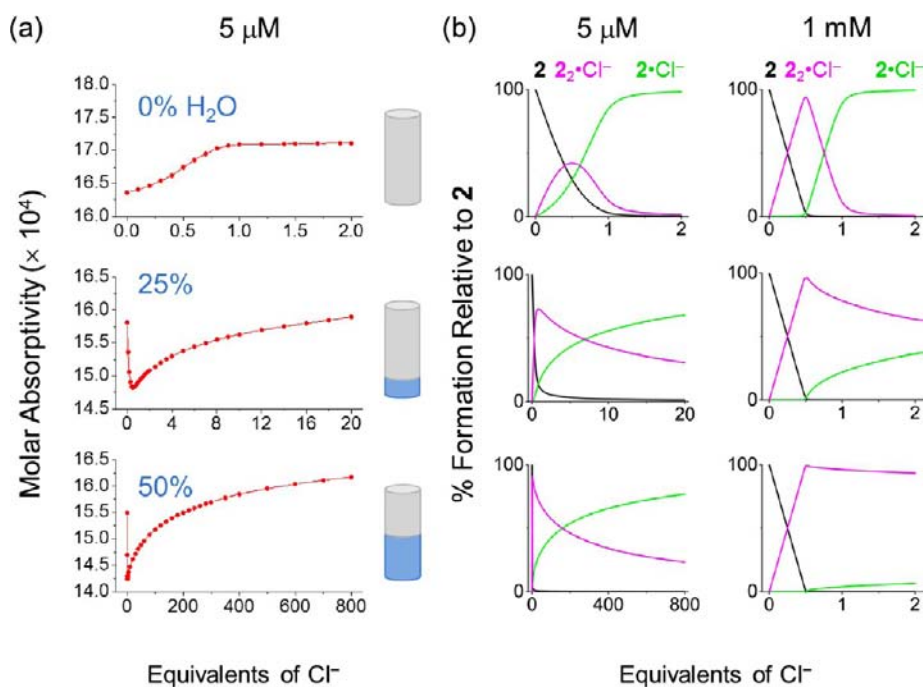
Figure 9. (a) Plots of the UV−vis changes measured at 260 nm during the titration of **2** with TBACl (5 μM, 293 K) in solutions containing 0%, 25%, and 50% water in MeCN. (b) Associated speciation curves calculated from the binding constants emphasize the distribution of species at 5 μM and 1 mM.

Table 1. Association Constants (K) and Free Energies (ΔG/kJ mol^{-1}) of Chloride-Binding Equilibria Involving Foldamer 2, Measured as a Function of Aqueous Content in MeCN at 293 K upon Addition of TBACl[a]

	0% water		25% water		50% water	
	K	ΔG	K	ΔG	K	ΔG
K_1	$(120 \pm 30) \times 10^6$ M^{-1} [b]	-46.0 ± 0.6	$(1.2 \pm 0.6) \times 10^6$ M^{-1}	-34.3 ± 1.5	$(0.23 \pm 0.06) \times 10^6$ M^{-1}	-30.6 ± 0.6
K_2	$(0.5 \pm 0.2) \times 10^6$ M^{-1}	-32 ± 1	$(3.8 \pm 2.0) \times 10^6$ M^{-1}	-37 ± 2	$(38 \pm 17) \times 10^6$ M^{-1}	-42.8 ± 1.0
β_2	$(60 \pm 15) \times 10^{12}$ M^{-2}	-78 ± 2	$(4.6 \pm 2.0) \times 10^{12}$ M^{-2}	-72.3 ± 3.5	$(9 \pm 5) \times 10^{12}$ M^{-2}	-73 ± 2
K_2/K_1	1/240	$+14 \pm 4$	3.2	-3 ± 5	165	-13 ± 2

[a]Titrations were duplicated at 0.5 and 5 μM. [b]K values in pure MeCN were determined by competitive titration against the more weakly bound dihydrogen phosphate ($H_2PO_4^-$, see Supporting Information)

system evolves almost directly from the empty foldamer to the 1:1 complex. The 1:1 species in pure MeCN is saturated at 1 equiv, while the more aqueous solution ultimately needs 400 equiv to access the single helix.

While duplexes are becoming increasingly studied,[62,64] double-helical complexes with bound anions are rare. These include Mendoza's bicyclic guanidiniums,[65] Martin's diamino-bis-pyridinium,[66] Gale's isophthalamides,[67] and Maeda's oligopyrroles.[68] By contrast to the aryl-triazole system examined here, these anion helicates have 2:2 stoichiometry, with two oligomers inter-twining together to form two separate binding sites suitable for capturing anions. In the first two examples,[65,66] charged receptors accommodated multiple anions within the binding cavity, while the latter three[67,68] were neutral. Furthermore, most of the duplexes were found in crystalline forms with molecular symmetries of C_2 or C_1, which may arise from higher crystal packing efficiencies of double helices compared to singles.[66,67,68a] In solution, either highly charged anions[65] or very low temperatures[68b] are required to form 2:2 helicates. Higher molecular symmetry, D_2, is observed in solution as a result of time-averaged screw motions.[62,69,70]

Solvent-Dependent Binding Constants. The similarity seen in the NMR ($\sim$1 mM) and CD (5 μM) titrations indicates that similar structures and equilibria are present across all solvent systems examined. Consequently, titration data collected using UV−vis spectroscopy were quantitatively analyzed according to a common set of equilibria:

$$\mathbf{2} + \text{Cl}^- \rightleftharpoons \mathbf{2}\cdot\text{Cl}^- \qquad K_1, \text{ overall 1:1 complex stability} \tag{1}$$

$$\mathbf{2}\cdot\text{Cl}^- + \mathbf{2} \rightleftharpoons \mathbf{2}_2\cdot\text{Cl}^- \qquad K_2, \text{ stepwise binding, duplex} \tag{2}$$

$$2\,\mathbf{2} + \text{Cl}^- \rightleftharpoons \mathbf{2}_2\cdot\text{Cl}^- \qquad \beta_2, \text{ overall 2:1 duplex stability} \tag{3}$$
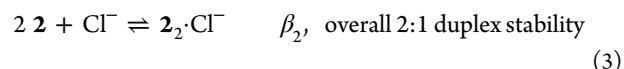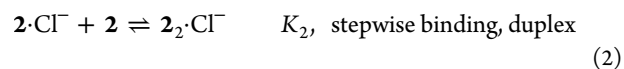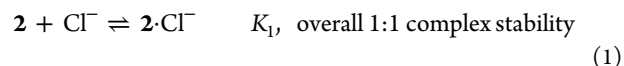
Use of low concentrations (0.5 and 5 μM duplicates) provided the weak binding conditions necessary[71] to accurately determine the equilibrium constants as well as excluding any effects that may arise from self-association (see Figure S30 for linearity of absorbance in 50:50 H$_2$O:MeCN, 0.8−58 μM).

The emergence of the duplex is seen clearly when inspecting how the primary UV−vis titration data (A_{260}, Figure 9a), the CD titration data (Figure 5), and the calculated speciation

curves (Figure 9b) change with increasing amounts of water. In pure MeCN, a modest point of inflection is observed at 0.5 equiv of chloride. This finding is consistent with the dominance of the $2 \cdot Cl^-$ complex relative to the $2_2 \cdot Cl^-$ duplex in MeCN alone. When the titration is repeated with 25% v/v of water in MeCN, the situation changes such that a clear inflection point is observed at 0.5 equiv, indicating the duplex's increasing importance. Consistently, 20 equiv of chloride now need to be added before the single helix $2 \cdot Cl^-$ is accessed in solution. With 50% water v/v, the situation intensifies such that the mass action of 800 equiv of chloride is required to form the $2 \cdot Cl^-$ complex after the $2_2 \cdot Cl^-$ duplex has been formed in this mixed aqueous solution. This behavior is characterized by a high degree of cooperativity (Table 1) between the two inter-twined foldamers within the duplex:

$$2 \; 2 \cdot Cl^- \rightleftharpoons 2_2 \cdot Cl^- + Cl^- \qquad K_2/K_1 \text{ cooperativity} \qquad (4)$$
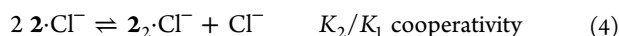
Relative to the single helix, $2 \cdot Cl^-$, the duplex becomes more stable upon the addition of water. This is the same signature observed by Kubik,[21c] and it shows unambiguously that hydrophobic interactions influence positively the stability of $2_2 \cdot Cl^-$ relative to $2 \cdot Cl^-$.

The impact of water on the three equilibria was characterized quantitatively (Table 1, Figure 10) by subjecting the data to
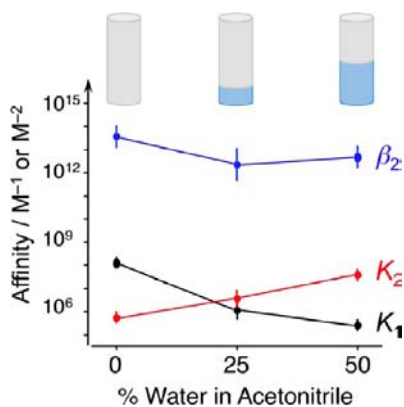
Figure 10. Plot of binding affinities (log scale) for foldamer **2** with Cl⁻ ions against the v/v percentage of water in MeCN for the equilibria K_1, K_2, and β_2 (see Table 1).

equilibrium-restricted factor analysis as implemented with Sivvu.[72] In pure MeCN, the 1:1 chloride affinity characterized by K_1 is unusually large, at $120{,}000{,}000 \text{ M}^{-1}$, and consequently it was determined by a competitive titration against dihydrogen phosphate, TBAH$_2$PO$_4$. This phosphate has an affinity of only $710{,}000 \text{ M}^{-1}$ (Supporting Information). The ^{1}H NMR titration with TBAH$_2$PO$_4$ (Figure S10) is almost identical to the one conducted with TBACl, consistent with the two complexes having similar geometries. Reflecting on the magnitude of the Cl⁻ affinity (log $K_1 = 8$), Maeda determined the same value from a pyrrolo foldamer bearing 15 hydrogen-bonding residues albeit in a less competitive solvent (dichloromethane, $\varepsilon = 9$) and when using a typical solvent-exposed pocket.[68a]

The 100-fold turn-off in the 1:1 chloride affinity (Figure 10, black line) displayed by **2** when changing from 0% to 25% water is dramatic, and, while this trend continues, there is a smaller 5-fold reduction in the affinity on going to 50% water. The decreasing affinities observed with the 1:1 complex are typical for the binding of hydrophilic guests in water. For instance, Kubik's oyster-like cyclopeptide receptors[21c] also

showed a turn-off effect toward the binding of sulfate in ~50–90% water in MeCN. This behavior is usually attributed to the increasing dehydration energy of guests, Cl⁻ ion in the present case. Nevertheless, the affinity obtained in 50% water, $K_1 = 230{,}000 \text{ M}^{-1}$, is still larger than that of other neutral receptors and comparable to that of the more competent charged receptors[15] under similar conditions, suggesting that solvent exclusion may play a beneficial role.

Hydrophobic interactions have a clear impact on the second equilibrium: the value of K_2 (Table 1) starts at $500{,}000 \text{ M}^{-1}$ in pure MeCN and increases to 3,800,000 and 38,000,000 M^{-1} in 25% and 50% water, respectively. The equilibrium can be described as an apolar binding process[12] where the partially organized foldamer **2** becomes inter-twined together[62] with the compact complex $2 \cdot Cl^-$. Consistently, the enhanced stability of the duplex in 50% water can be rationalized from the total number of π surfaces that are buried (Figure 11). Each
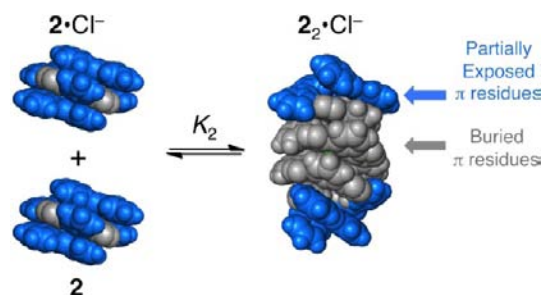
Figure 11. Molecular models showing the buried π surfaces in the single and double helices. Space-filling models of the foldameric species involved in equilibrium K_2 using color to distinguish the residues that are partially solvent exposed (blue) from the ones that are completely buried (gray). Side chains and hydrogen atoms have been removed for clarity.

foldamer has 15 residues with nine phenyls and six triazoles. Each foldamer has a top and bottom face constituting 30 π surfaces. With two foldamers present on either side of equilibrium K_2, there are 60 π surfaces in total. A model of the double helix shows that ~80% of the total π surfaces get buried upon complex formation; the gray color in Figure 11 corresponds to the residues that have *both* their top and bottom faces hidden. By contrast, the crystal structure of $1^* \cdot Cl^- \cdot Na^+$ shows that only ~50% of its π surfaces are buried. The empty foldamer is not completely folded at room temperature and on average is expected to have an even smaller number of buried π surfaces than the 1:1 complex. Therefore, the duplex has a significant advantage by being able to bury more π surfaces as the solvent composition gains aqueous content. This phenomenon exemplifies the IUPAC definition of hydrophobic interactions: *the tendency of hydrocarbon-like solutes to form intermolecular aggregates in an aqueous medium and analogous intramolecular interactions.*[73]

As a result of the hydrophobic interaction, the overall stability of the duplex (β_2) changes very little upon addition of water: β_2 varies within an order of magnitude across the series (Table 1). The net stability of the duplex can be explained from its constituent equilibria, $K_1 \times K_2 = \beta_2$. The penalty of Cl⁻ dehydration is first paid in equilibrium K_1, yet this penalty is offset by the effect of hydrophobicity on equilibrium K_2: the equilibria (Figure 10) shift in almost equal but opposite directions as the aqueous content increases. The impact of hydrophobicity is so strong that it almost counteracts the
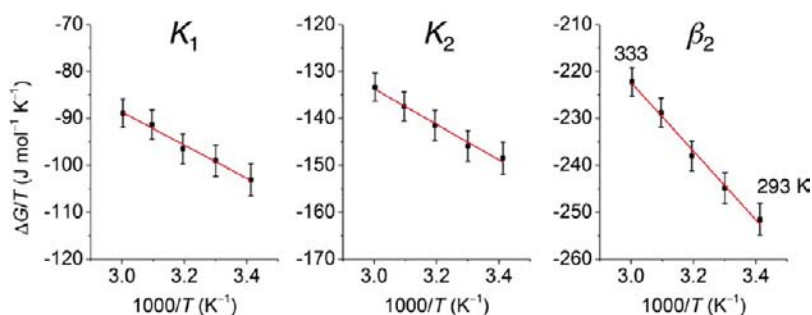
Figure 12. van't Hoff analyses (293−313 K) of the stepwise 1:1 binding (K_1), stepwise 2:1 binding (K_2), and overall 2:1 duplex formation (β_2) equilibria for foldamer **2** in 50:50 H$_2$O:MeCN measured at 5 μM using a UV−vis titration.

Table 2. Thermodynamic Quantities for Chloride Binding with Foldamer 2, Determined in 50% Water/Acetonitrile at Different Temperatures (293−333 K)

	ΔG/kJ mol^{-1}, 293 K	ΔH/kJ mol^{-1}	$-T\Delta S$/kJ mol^{-1}, 293 K	ΔS/J K^{-1} mol^{-1}
2 + Cl$^-$ ⇌ **2**·Cl$^-$	−30.2 ± 0.5	−35 ± 2	5 ± 2	−17 ± 7
2 + **2**·Cl$^-$ ⇌ **2**$_2$·Cl$^-$	−43.5 ± 0.5	−38 ± 2	−6 ± 2	20 ± 8
2 **2** + Cl$^-$ ⇌ **2**$_2$·Cl$^-$	−73.7 ± 0.5	−73 ± 3	−1 ± 3	3 ± 11

penalty of desolvation. This behavior is unprecedented in the binding of hydrophilic anions like chloride or sulfate.[15]

Concomitant with hydrophobic collapse, solvent molecules are also excluded from the buried π surfaces. We postulate this solvent exclusion phenomenon may play a positive role in the creation of a microenvironment that favors anion binding in the duplex over the single helix. The crystal structure of the complex **1***·Cl$^-$·Na$^+$ provides a basis to examine this idea. With only 50% of the π surfaces in a single foldamer buried, half of them are still exposed to solvent (blue residues in Figure 11). Focusing on the stronger hydrogen bonds from the triazoles, all six of them have one of their two faces involved in forming a π-stacked seam, i.e., buried. Considering the more exposed faces, the azobenzene cap may be the primary source of solvent exclusion. It partially covers two of the triazoles, and it does a good job of wrapping up the central Cl$^-$ ion and protecting the H···Cl$^-$ contact regions of the hydrogen bond. However, the remaining four triazoles are totally exposed to solvent. A completely different situation is present within our model of the double helix (Figure 11). All the triazoles engaging with a centrally located Cl$^-$ ion have their π faces and their CH···Cl$^-$ hydrogen bonds buried; only the triazole nitrogens are available for solvation. The hydrogen bonds inside **2**$_2$·Cl$^-$ are therefore expected to be stronger than those in **2**·Cl$^-$. This positive factor will contribute to enhancing the stability of the duplex relative to the single helix, an additional driving force favoring the products in equilibrium K_2. Moreover, the formation of a hydrogen bond may reduce the local dipole on the triazoles, providing more apolar π surfaces to synergistically enhance further the hydrophobic interactions in a manner akin to proteins.[74,75] While the *cis*-to-*trans* ratio of the UV photostationary state was low,[43g,51,59] the 1:1 affinity for Cl$^-$ in MeCN was found to be reduced by 5 kJ mol^{-1} (Table S2), an observation consistent with solvent accessing the binding environment after the azobenzene gate is opened.

Thermodynamics of Binding in Aqueous Solution. The thermodynamics of the equilibria helped provide further insights into the driving forces at play in the mixed 50:50 aqueous solution. First, the change in the free energies for the chloride-binding reaction K_1 as a function of solvent content (Table 1) is not linear. This observation indicates that more

than one factor is varying with the solution composition, an interpretation consistent with solvent-dependent studies of folding in helical peptides.[76] Second, van't Hoff plots (293−333 K, Figure 12) show that all equilibria are enthalpy driven (Table 2), such that the free energy of the reaction can be largely accounted for by enthalpy alone. The entropy contribution to these reactions in 50% water is negligible. Isothermal titration calorimetry was conducted in 50% water at 293 K (see Figure S28) to verify this result. At the concentration examined (25 μM), the solution speciates almost exclusively into the 2:1 species. Consistently, addition of ∼0.5 equiv gives a large exothermic response leading to formation of the duplex, $\Delta H(\beta_2)_{293} = -76$ kJ mol^{-1}, a value matching the van't Hoff analysis.

Considering the origin of this thermodynamic profile, the entropic benefits of freeing up water molecules from around the apolar surfaces of the foldamers (K_1, K_2, and β_2) and from the chloride (K_1 and β_2) are presumably offset by the penalty of freezing the conformational and rotational space when the foldamers are locked up into complexes (K_1, K_2, and β_2). The enthalpic driving forces are expected to benefit from formation of CH···Cl$^-$ hydrogen bonds (K_1 and β_2), as well as any strengthening of the hydrogen bonds as a consequence of the microenvironment in the duplex (K_2) and the π−π interactions (K_1, K_2, and β_2). Diederich[53,77,78] and others[79] observed enthalpy-driven equilibria in apolar binding events, with entropy playing a smaller role. This outcome was considered a nonclassical signature of the hydrophobic effect by Diederich[12] and by Dill as a more general feature of solvophobic interactions,[80] where the hydrophobic effect is a special case seen in some but not all binding phenomena involving water. On the basis of these works, the release of water molecules also involves an enthalpic benefit in that those waters may have a greater number of hydrogen bonds with each and that these will be stronger interactions. All of these factors will offset the enthalpic penalty associated with dehydration/desolvation of Cl$^-$ ions.

■ CONCLUSIONS

Hydrophobic interactions provide a significant driving force in stabilizing folded aryl-triazole complexes to facilitate the

extraction of chloride from increasingly aqueous environments, in direct opposition to the impact of that additional water on hydrating the chloride ion. The burial of ∼80% of the hydrophobic π surfaces in the duplex distinguishes its behavior from that of the single helix, which only buries ∼50%. Shielding of hydrogen-bond donors from solvent within the complex is aided by the azobenzene caps in the single helix and by π stacking of the main chain in the duplex, which is believed to create a more potent microenvironment. Thus, within these foldamers, hydrophobic interactions are proposed to pay the energetic cost of stabilizing and partially organizing the duplex to help define a solvent-excluding cavity capable of generating stronger CH···Cl⁻ hydrogen bonds for the extraction of chloride from an increasingly competitive aqueous environment. While the performance of these helical foldamers is not yet perfect, the analogy to proteins is striking (Figure 13):
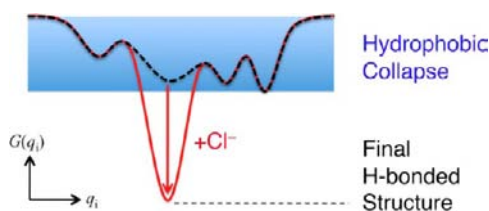
Figure 13. Biomimetic energy surface reflecting hydrophobic collapse and the formation of a final discrete structure for foldamers 1* and 2 before (black line) and after (red line) binding Cl⁻.

hydrophobic collapse cooperates with hydrogen bonds to generate a final organized structure. The continuing establishment of rules guiding the design of foldamers could facilitate the application of this biomimetic strategy in the capture of other polar guests.

■ METHODS

See Supporting Information for detailed experimental conditions and procedures, syntheses and compound characterizations, single-crystal X-ray structure with CCDC no. 888675, ¹H NMR spectroscopic analyses, titration data and analyses, CD spectroscopy, temperature-dependence and ITC data, photoisomerization analysis, and variable concentration studies.

■ ASSOCIATED CONTENT

Ⓢ Supporting Information
Syntheses, additional NMR data (1D and 2D), crystal structures, UV−vis data, CD data, and ITC data. This material is available free of charge via the Internet at http://pubs.acs.org.

■ AUTHOR INFORMATION

Corresponding Author
aflood@indiana.edu

Notes
The authors declare no competing financial interest.

■ ACKNOWLEDGMENTS

■ REFERENCES

(1) Pedersen, C. J. *J. Am. Chem. Soc.* **1967**, *89*, 7017−7036.
(2) Lehn, J.-M. *Angew. Chem., Int. Ed.* **1988**, *27*, 89−112.
(3) Cram, D. J. *Angew. Chem., Int. Ed.* **1986**, *25*, 1039−1057.
(4) Rekharsky, M. V.; Mori, T.; Yang, C.; Ko, Y. H.; Selvapalam, N.; Kim, H.; Sobransingh, D.; Kaifer, A. E.; Liu, S.; Isaacs, L.; Chen, W.; Moghaddam, S.; Gilson, M. K.; Kim, K.; Inoue, Y. *Proc. Natl. Acad. Sci. U.S.A.* **2007**, *52*, 20737−20742.
(5) Cox, B. G.; Garcia-Rosas, J.; Schneider, H. *J. Am. Chem. Soc.* **1981**, *103*, 1384−1389.
(6) Fan, E.; Van Arman, S. A.; Kincaid, S.; Hamilton, A. D. *J. Am. Chem. Soc.* **1993**, *115*, 369−370.
(7) Kearney, P. C.; Mizoue, L. S.; Kumpf, R. A.; Forman, J. E.; McCurdy, A.; Dougherty, D. A. *J. Am. Chem. Soc.* **1993**, *115*, 9907−9919.
(8) Gunnlaugsson, T.; Glynn, M.; Tocci, G. M.; Kruger, P. E.; Pfeffer, F. M. *Coord. Chem. Rev.* **2006**, *250*, 3094−3117.
(9) Hirschberg, J. H. K. K.; Brunsveld, L.; Ramzi, A.; Vekemans, J. A. J. M.; Sijbesma, R. P.; Meijer, E. W. *Nature* **2000**, *407*, 167−170.
(10) Lokey, R. S.; Iverson, B. L. *Nature* **1995**, *375*, 303−305.
(11) Ma, D.; Hettiarachchi, G.; Nguyen, D.; Zhang, B.; Wittenberg, J. B.; Zavalij, P. Y.; Volker, B.; Isaacs, L. *Nat. Chem.* **2012**, *4*, 503−510.
(12) Meyer, E. A.; Castellano, R. K.; Diederich, F. *Angew. Chem., Int. Ed.* **2003**, *42*, 1210−1250.
(13) Diederich, F. *Angew. Chem., Int. Ed.* **1988**, *27*, 362−386.
(14) *Physiology and pathology of chloride transporters and channels in the nervous system*; Alvarez-Leefmans, F. J., Delpire, E., Eds.; Academic Press: New York, 2009.
(15) Kubik, S. *Chem. Soc. Rev.* **2010**, *39*, 3648−3663.
(16) Dietrich, B.; Hosseini, M. W.; Lehn, J.-M.; Sessions, R. B. *J. Am. Chem. Soc.* **1981**, *103*, 1282−1283.
(17) Cai, J.; Hay, B. P.; Young, N. J.; Yang, X.; Sessler, J. L. *Chem. Sci.* **2013**, *4*, 1560−1567.
(18) White, N. G.; Carvalho, S.; Felix, V.; Beer, P. D. *Org. Biomol. Chem.* **2012**, *10*, 6951−6959.
(19) Kubik, S.; Goddard, R.; Kirchner, R.; Nolting, D.; Seidel, J. *Angew. Chem., Int. Ed.* **2001**, *40*, 2648−2651.
(20) (a) Suk, J.-M; Jeong, K.-S. *J. Am. Chem. Soc.* **2008**, *130*, 11868−11869. (b) Juwarker, H.; Jeong, K.-S. *Chem. Soc. Rev.* **2010**, *39*, 3664−3674.
(21) (a) Kubik, S.; Goddard, R. *Proc. Natl. Acad. Sci. U.S.A.* **2002**, *99*, 5127−5132. (b) Kubik, S.; Kirchner, R.; Nolting, D.; Seidel, J. *J. Am. Chem. Soc.* **2002**, *124*, 12752−12760. (c) Rodriguez-Docampo, Z.; Pascu, S. I.; Kubik, S.; Otto, S. *J. Am. Chem. Soc.* **2006**, *128*, 11206−11210. (d) Kubik, S. *Chem. Soc. Rev.* **2010**, *39*, 3648−3663.
(22) Nicholls, A.; Sharp, K. A.; Honig, B. *Proteins: Struct., Funct. Genet.* **1991**, *11*, 281−296.
(23) Hydrophobic cores of proteins produce microenvironments in which the magnitude of the suppression in ε is not easy to quantify. Static dielectric constants of dry protein powders range from 2 to 4; see ref 24. Recent work using changes in acidity give values as high as 12 and relate the reduction in the local dielectric constant to lower levels of water penetration; see ref 25.
(24) Harvey, S. C.; Hoekstra, P. *J. Phys. Chem.* **1972**, *76*, 2987−2994.
(25) Dwyer, J. J.; Gittis, A. G.; Karp, D. A.; Lattman, E. E.; Spencer, D. S.; Stites, W. E.; Garcia-Moreno, E., B. *Biophys. J.* **2000**, *79*, 1610−1620.
(26) Jeffrey, G. A. *An introduction to hydrogen bonding*; Oxford University Press: New York, 1997.
(27) Moyer, B. A.; Bonnesen, P. V. In *Supramolecular chemistry of anions*; Bianchi, A., Bowman-James, K., Garcia-Espana, E., Eds.; Wiley-VCH: Weinheim, 1997.

(28) The transfer energies from water to 1,2-dichloroethane for I⁻ and ClO₄⁻ are 26 and 17 kJ mol⁻¹, respectively, whereas for Cl⁻ it is 46 kJ mol⁻¹; see ref 27.

(29) Hofmeister, F. *Arch. Exp. Pathol. Pharmakol.* **1888**, *24*, 247−260.

(30) Zhang, Y.; Cremer, P. S. *Annu. Rev. Phys. Chem.* **2010**, *61*, 63−83.

(31) Gibb, C. L. D.; Gibb, B. C. *J. Am. Chem. Soc.* **2011**, *133*, 7344−7347.

(32) Pflugrath, J. W.; Quiocho, F. A. *Nature* **1985**, *314*, 257−260.

(33) Jentsch, T. J.; Stein, V.; Weinreich, F.; Zdebik, A. A. *Physiol. Rev.* **2002**, *82*, 503−568.

(34) Dutzler, R.; Campbell, E. B.; Cadene, M.; Chait, B. T.; MacKinnon, R. *Nature* **2002**, *415*, 287−294.

(35) *Foldamers: Structure, properties and applications*; Hecht, S., Huc, I., Eds.; Wiley-VCH: Weinheim, 2007.

(36) Nelson, J. C.; Saven, J. G.; Moore, J. S.; Wolynes, P. G. *Science* **1997**, *277*, 1793−1796.

(37) Prince, R. B.; Barnes, S. A.; Moore, J. S. *J. Am. Chem. Soc.* **2000**, *122*, 2758−2762.

(38) Saraogi, I.; Hamilton, A. D. *Chem. Soc. Rev.* **2009**, *38*, 1726−1743.

(39) Inouye, M.; Waki, M.; Abe, H. *J. Am. Chem. Soc.* **2004**, *126*, 2022−2027.

(40) (a) Juwarker, H.; Suk, J.-M.; Jeong, K.-S. *Chem. Soc. Rev.* **2009**, *38*, 3316−3325. (b) Juwarker, H.; Jeong, K.-S. *Chem. Soc. Rev.* **2010**, *39*, 3664−3674.

(41) Li, X.; Wu, Y.-D.; Yang, D. *Acc. Chem. Res.* **2008**, *41*, 1428−1438.

(42) Garric, J.; Léger, J.-M.; Huc, I. *Angew. Chem., Int. Ed.* **2005**, *44*, 1954−1958.

(43) (a) Li, Y.; Flood, A. H. *Angew. Chem., Int. Ed.* **2008**, *47*, 2649−2652. (b) Li, Y.; Flood, A. H. *J. Am. Chem. Soc.* **2008**, *130*, 12111−12122. (c) Li, Y.; Pink, M.; Karty, J. A.; Flood, A. H. *J. Am. Chem. Soc.* **2008**, *130*, 17293−17295. (d) Li, Y.; Vander Griend, D. A.; Flood, A. H. *Supramol. Chem.* **2009**, *21*, 111−117. (e) Bandyopadhyay, I.; Raghavachari, K.; Flood, A. H. *ChemPhysChem* **2009**, *10*, 2535−2540. (f) Lee, S.; Hua, Y.; Park, H.; Flood, A. H. *Org. Lett.* **2010**, *12*, 2100−2101. (g) Hua, Y.; Flood, A. H. *J. Am. Chem. Soc.* **2010**, *132*, 12838−12840. (h) Hua, Y.; Ramabhadran, R. O.; Uduehi, E. O.; Karty, J. A.; Raghavachari, K.; Flood, A. H. *Chem.—Eur. J.* **2011**, *17*, 312−321. (i) Hua, Y.; Ramabhadran, R. O.; Karty, J. A.; Raghavachari, K.; Flood, A. H. *Chem. Commun.* **2011**, *47*, 5979−5981. (j) Ramabhadran, R. O.; Hua, Y.; Flood, A. H.; Raghavachari, K. *Chem.—Eur. J.* **2011**, *17*, 9123−9129. (k) McDonald, K. P.; Ramabhadran, R. O.; Lee, S.; Raghavachari, K.; Flood, A. H. *Org. Lett.* **2011**, *13*, 6260−6263. (l) McDonald, K. P.; Hua, Y.; Lee, S.; Flood, A. H. *Chem. Commun.* **2012**, *48*, 5065−5075. (m) Lee, S.; Flood, A. H. *J. Phys. Org. Chem.* **2013**, *26*, 97−86.

(44) You, L.-Y.; Chen, S.-G.; Zhao, X.; Liu, Y.; Lan, W.-X.; Zhang, Y.; Lu, H.-J.; Cao, C.-Y.; Li, Z.-T. *Angew. Chem., Int. Ed.* **2012**, *51*, 1657−1661.

(45) Wang, Y.; Xiang, J.; Jiang, H. *Chem.—Eur. J.* **2011**, *17*, 613−619.

(46) Lu, B.-Y.; Li, Z.-M.; Zhu, Y.-Y.; Zhao, X.; Li, Z.-T. *Tetrahedron* **2012**, *68*, 8857−8862.

(47) Juricek, M.; Kouwer, P. H. J.; Rowan, A. E. *Chem. Commun.* **2011**, *47*, 8740−8749.

(48) Zornik, D.; Meudtner, R. M.; Malah, T. E.; Thiele, C. M.; Hecht, S. *Chem.—Eur. J.* **2011**, *17*, 1473−1484.

(49) Suk, J.; Kim, D. A.; Jeong, K.-S. *Org. Lett.* **2012**, *14*, 5018−5021.

(50) Kim, M. J.; Lee, H.-W.; Moon, D.; Jeong, K.-S. *Org. Lett.* **2012**, *14*, 5042−5045.

(51) Meudtner, R. M.; Hecht, S. *Angew. Chem., Int. Ed.* **2008**, *47*, 4926−4930.

(52) Wang, Y.; Li, F.; Han, Y. M.; Wang, F. Y.; Jiang, H. *Chem.—Eur. J.* **2009**, *15*, 9424−9433.

(53) Smithrud, D. B.; Sanford, E. M.; Chao, I.; Ferguson, S. B.; Carcanague, D. R.; Evanseck, J. D.; Houk, K. N.; Diederich, F. *Pure Appl. Chem.* **1990**, *62*, 2227−2236.

(54) Sessler, J. L.; Gale, P. A.; Cho, W.-S. *Anion receptor chemistry*; RSC Publishing: London, 2006.

(55) *Bioinspiration and Biomimicry in Chemistry: Reverse Engineering Nature*; Swiegers, G. F., Ed.; Wiley: Hoboken, NJ, 2012.

(56) (a) Hua, Y.; Flood, A. H. *Chem. Soc. Rev.* **2010**, *39*, 1262−1271. (b) Lee, S.; Chen, C.-H.; Flood, A. H. *Nat. Chem.* **2013**, *5*, 704−710.

(57) Bryantsev, V. D.; Hay, B. P. *J. Am. Chem. Soc.* **2005**, *127*, 8282−8283.

(58) Yu, Z.; Hecht, S. *Angew. Chem., Int. Ed.* **2011**, *50*, 1640−1643.

(59) Khan, A.; Kaiser, C.; Hecht, S. *Angew. Chem., Int. Ed.* **2006**, *45*, 1878−1881.

(60) Suk, J.; Naidu, V. R.; Liu, X.; Lah, M. S.; Jeong, K.-S. *J. Am. Chem. Soc.* **2011**, *133*, 13938−13941.

(61) Juwarker, H.; Lenhardt, J. M.; Pham, D. M.; Craig, S. L. *Angew. Chem., Int. Ed.* **2008**, *47*, 3740−3743.

(62) Berl, V.; Huc, I.; Khoury, R. G.; Krische, M. J.; Lehn, J.-M. *Nature* **2000**, *407*, 720−723.

(63) Kim, S. K.; Sessler, J. L. *Chem. Soc. Rev.* **2010**, *39*, 3784−3809.

(64) (a) Piguet, C.; Bernardinelli, G.; Hopfgartner, G. *Chem. Rev.* **1997**, *97*, 2005. (b) Swiegers, G. F.; Malefetse, T. J. *Chem. Rev.* **2000**, *100*, 3483−3537. (c) Albrecht, M. *Chem. Rev.* **2001**, *101*, 3457. (d) Maurizot, V.; Léger, J. M.; Guionneau, P.; Huc, I. *Russ. Chem. B* **2004**, *53*, 1572−1576. (e) Guido, H. C.; Corinna, K.; Thomas, C. *Angew. Chem., Int. Ed.* **2007**, *46*, 6226−6236. (f) Haldar, D.; Schmuck, C. *Chem. Soc. Rev.* **2009**, *38*, 363−371. (g) Furusho, Y.; Yashima, E. *Macromol. Rapid Commun.* **2011**, *32*, 136−146.

(65) Sánchez-Quesada, J.; Seel, C.; Prados, P.; de Mendoza, J.; Dalcol, I.; Giralt, E. *J. Am. Chem. Soc.* **1996**, *118*, 277−278.

(66) Keegan, J.; Kruger, P. E.; Nieuwenhuyzen, M.; O'Brien, J.; Martin, N. *Chem. Commun.* **2001**, 2192−2193.

(67) Coles, S. J.; Frey, J. G.; Gale, P. A.; Hursthouse, M. B.; Light, M. E.; Navakhun, K.; Thomas, G. L. *Chem. Commun.* **2003**, 568−569.

(68) (a) Haketa, Y.; Maeda, H. *Chem.—Eur. J.* **2011**, *17*, 1485−1492. (b) Maeda, H.; Kitaguchi, K.; Haketa, Y. *Chem. Commun.* **2011**, *47*, 9342−9344.

(69) Acocella, A.; Venturini, A.; Zerbetto, F. *J. Am. Chem. Soc.* **2004**, *126*, 2362−2367.

(70) Maurizot, V.; Léger, J. M.; Guionneau, P.; Huc, I. *Russ. Chem. B* **2004**, *53*, 1572−1576.

(71) Hirose, K. In *Analytical Methods in Supramolecular Chemistry*; Schalley, C. A., Ed.; Wiley-VCH: Weinheim, 2007.

(72) Vander Griend, D. A.; Bediako, D. K.; DeVries, M. J.; DeJong, N. A.; Heeringa, L. P. *Inorg. Chem.* **2007**, *47*, 656−662.

(73) IUPAC. *Compedium of Chemical Terminology*, 2nd ed.; McNaught, A. D., Wilkinson, A., Eds.; Blackwell Scientific Publications: Oxford, 1997.

(74) Rernandez, A.; Kardos, J.; Goto, Y. *FEBS Lett.* **2003**, *536*, 187−192.

(75) Fernandez, A.; Crespo, A. *Chem. Soc. Rev.* **2008**, *37*, 2373−2382.

(76) Albert, J. S.; Hamilton, A. D. *Biochemistry* **1995**, *34*, 984−990.

(77) Ferguson, S. B.; Seward, E. M.; Diederich, F.; Sanford, E. M.; Chou, A.; Inocencio-Szweda, P.; Knobler, C. B. *J. Org. Chem.* **1988**, *53*, 5593−5595.

(78) Smithrud, D. B.; Wyman, T. B.; Diederich, F. *J. Am. Chem. Soc.* **1991**, *113*, 5420−5426.

(79) Harata, K.; Tsuda, K.; Uekama, K.; Otagiti, M.; Hirayama, F. *J. Inclusion Phenom.* **1988**, *6*, 135−142.

(80) Southall, N. T.; Dill, K. A. *J. Phys. Chem. B* **2000**, *104*, 1326−1331.